Stopping power of fast protons under channeling conditions

K. Dettmann and M. T. Robinson*
Institut für Festkörperforschung der Kernforschungsanlage Jülich, 517 Jülich, West Germany
(Received 15 October 1973)

For fast channeled protons the electronic stopping power S_c is investigated in an impact-parameter treatment, where, for single inelastic atomic collisions, the proton moves on a classical straight-line trajectory. The electrons of the crystal atoms are described by hydrogenlike wave functions. In the MeV-energy range, the Born approximation can be applied. An average over all impact parameters yields a mean electronic excitation energy per collision that is twice the binding energy. Using this average for each impact parameter separately, we obtain S_c, slowly varying and finite for close collisions and with a long-range part corresponding to distant collisions. The results are in good agreement with experimental data in Si and Ge.

I. INTRODUCTION

In the MeV-energy range, protons passing through matter rapidly with respect to the atomic electrons suffer small-angle deflections by nuclear collisions, have a negligible chance to pick up an electron, and lose kinetic energy E by electronic excitation and ionization. The average energy loss per unit path length, the electronic stopping power $S_r = -dE/dx$, is well described by the Bethe-Bloch formula,[1] as long as the proton moves through a random arrangement of atoms. In a crystal, however, protons can be injected in low-index crystallographic directions, moving along open axes or planes and avoiding close collisions with the crystal atoms (Fig. 1). For such a channeling situation, the Bethe-Bloch treatment no longer applies, since small-impact parameters $b_m \ll \frac{1}{2}a$ (Fig. 1) are avoided.

To account for the channel stopping power S_c, Lindhard[2] referred to his dielectric approach for the energy loss of protons in a free-electron gas. This model yields, for fast protons, equipartition of S_r into collisions with small momentum transfer, or plasmon excitation, and those with large momentum transfer, or single-particle excitation. For a channeling situation with only distant collisions, Lindhard excludes single-particle excitation, since he assumes this to be proportional to the local electron density $n(\vec{r}) \cong 0$. Then the stopping power S_c for fast channeled protons should be reduced to one half of the random Bethe-Bloch value, in contradiction to the experimental results in Ge.[3]

In Bloch's impact-parameter treatment,[4-6] the inelastic energy loss is calculated in a first Born approximation for the model of single collisions with hydrogenlike atoms. An energy- and impact-parameter-independent excitation energy is assumed equal to the binding energy $|\epsilon_0|$ of the electron shell under consideration. The average energy loss $\Delta E(b_m, E)$, due to a collision with the crystal atom m (Fig. 1), is calculated in the dipole approximation, valid for $b \gg a_0$, where a_0 is the scaled Bohr radius. For impact parameters $b \leq a_0$, $\Delta E(b, E)$ is extrapolated, supplying unphysically large values for small b with a $1/b^2$ divergence at $b = 0$. This is corrected artificially by introducing a cutoff impact parameter b', so that the integral over $b \geq b'$ yields the random Bethe-Bloch value S_r/ρ, where ρ is the density of atoms.

Our approach is based on the same atomic collision model as Bloch's. In contrast to his calculation we avoid the dipole approximation, so that small-impact parameters also are included, which occur for protons with large oscillation amplitudes in Fig. 1. The wavelength of the trajectories is always many lattice constants so that a straight-line assumption for each individual collision is valid even for large oscillation amplitudes. Like Bloch, we keep the first Born approximation and an approximately impact-parameter-independent excitation energy. But this is calculated self-consistently and results in $2|\epsilon_0|$ for large proton velocity. Compared with former results[4-6] we obtain, for $b > a_0$, a larger energy loss of shorter but still long range, while $\Delta E(b < a_0)$ is slowly varying and stays finite at $b = 0$.

We apply our results to proton channeling in Si and Ge and obtain good agreement with the experimental data. In particular, we explain quantitatively the different ratios $R = S_c/S_r$ for Si and Ge.

II. THEORY

The stopping power of the channeled proton in Fig. 1 is

$$S_c(x) = -\frac{dE}{dx} = \frac{1}{a}\sum_m \Delta E[b_m(x), v] , \tag{1}$$

where $\Delta E(b_m, v)$ is the average energy loss due to the collision with the crystal atom m at a distance x from the surface, when the proton of velocity v passes with impact parameter b_m. The sum ex-

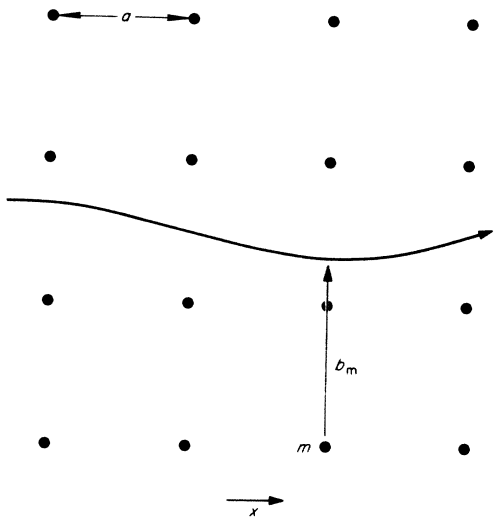

FIG. 1. Channeled proton trajectory (schematic for axial channeling in a simple cubic lattice with lattice constant a).

tends over all lattice sites m in a plane perpendicular to the particle trajectory, and a is the lattice constant. The random-stopping power S_r results from (1) by averaging S_c over the channel cross section $F = a^2$:

$$S_r = \frac{1}{F}\int_F df\, S_c = \frac{1}{Fa}\sum_m \int_F d^2b_m\, \Delta E(\vec{b}_m, v) = \rho \int_\infty d^2b\, \Delta E(\vec{b}, v) \ . \tag{2}$$

In (2) ρ is the density of atoms in the crystal, and the last integral extends over all $\vec{b}$. We calculate $\Delta E(\vec{b}, v)$ in the model of Fig. 2.

The proton p moves with impact parameter $\vec{b}$ and velocity $\vec{v}$ on a straight-line trajectory $\vec{R}(t) = \vec{b} + \vec{v}t$ past an atom of atomic number Z. The curvature of the trajectory can be neglected for each atomic collision, since the wavelength of the trajectory in the channel extends over many lattice constants. Each electron i of mass m and charge $-e$ is described by a hydrogen model and assumed to be bound by an effective Coulomb potential $V_i = -Z_i e^2/r$ in a hydrogenlike ground state $|0\rangle_i$ with the energy ϵ_0^i. The binding energy $-\epsilon_0^i$ is the ionization potential of electron i and determines the effective Z_i. The time-dependent Coulomb interaction $V(r' = |\vec{r} - \vec{R}(t)|) = -e^2/r'$ causes transitions of i from $|0\rangle_i$ to excited or ionized states $|n\rangle_i$ with energies ϵ_n^i corresponding to energy losses $\epsilon_n^i - \epsilon_0^i$ of the proton. The average energy loss ΔE^i due to electron i can then be summed incoherently to yield

$$\Delta E(b, v) = \sum_i \Delta E^i(b, v) \ . \tag{3}$$

By (3) the calculation of the channel stopping power (1) is reduced to evaluating the average inelastic energy loss for a proton-hydrogen collision in the impact-parameter treatment with scaled charge Z_i.

Considering only one electron in the following, we drop for convenience the index i. The average inelastic energy loss is

$$\Delta E(b, v) = \hbar \sum_{n>0} (\omega_n - \omega_0) P_n(\vec{b}, v), \quad \hbar\omega_n = \epsilon_n \ , \tag{4}$$

where $P_n(\vec{b}, v)$ is the transition probability for exciting the electron to a state $|n\rangle$ in the collision of Fig. 2. The cross section for this process is

$$\sigma_n = \int P_n(\vec{b}, v) d^2\vec{b} \ . \tag{5}$$

The transition probability can be calculated by

$$P_n(\vec{b}, v) = |f_n(\vec{b}, v)|^2, \quad f_n = \langle n | \psi(t \to \infty) \rangle \ , \tag{6}$$

where $\psi(t)$ is the electronic state at time t, developing from the initial state $|\psi(t \to -\infty)\rangle = |0\rangle e^{-i\omega_0 t}$ according to the Schrödinger equation

$$H|\psi\rangle = i\hbar|\dot{\psi}\rangle, \quad H = -(\hbar^2/2m)\nabla^2 + V_i(r) + V(\vec{r} - \vec{R}(t)) \ . \tag{7}$$

After some operator algebra[7] one obtains for the amplitude

$$f_n = -(i/\hbar)\int_{-\infty}^{\infty} dt\, e^{i\omega_n t} \langle n | V(t) | \psi(t) \rangle \ . \tag{8}$$

Since we are dealing with fast protons, we have $v \gg v_0$ for the outer electrons, $v_0 = \hbar/a_0 m$ being the orbital electron velocity. Then the collision time is short and $V(t)$ can be considered as a small perturbation applied to $|0\rangle$. The inner electrons are strongly bound, and V is small compared with V_i, so that again a perturbation treatment is sufficient. We therefore evaluate f_n in (8) in a first Born approximation, replacing $\psi(t)$ by the unperturbed ground state, and obtain

$$f_n \cong -(i/\hbar)\int_{-\infty}^{\infty} dt\, e^{i(\omega_n - \omega_0)t} \langle n | V(t) | 0 \rangle \ . \tag{9}$$

Introducing (9) and (6) into (4) yields a sum over n, which is hard to perform exactly. We therefore approximate $\omega_n - \omega_0$ by $\bar{\omega}(v)$, which is independent of n and is calculated self-consistently by averaging over all impact parameters b with (2) and (5). The sum can then be performed by the closure re-

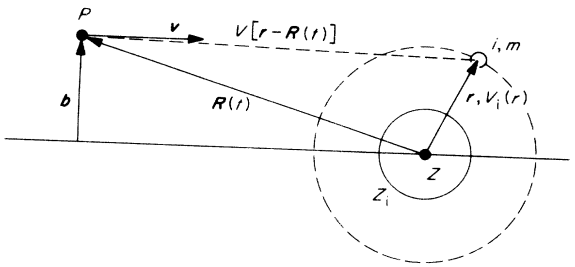

FIG. 2. Hydrogenlike model for a proton-atom collision.

lation with the result

$$\Delta E(b, v) \cong \Delta E_{\bar{\omega}}(b, v) , \tag{10}$$

where

$$\Delta E_{\bar{\omega}} = (\bar{\omega}/\hbar)\{\langle 0| \, |V(\bar{\omega}, b)|^2 |0\rangle - |\langle 0| V(\bar{\omega}, b)|0\rangle|^2\} ,$$

$$V(\bar{\omega}, b) = \int dt\, e^{i\bar{\omega}t} V(t) = -e^2 \int dt \, \frac{e^{i\bar{\omega}t}}{|\vec{r} - \vec{v}t - \vec{b}|}$$

$$= -\frac{2e^2}{v} e^{i(\bar{\omega}/v)x} K_0\left(\frac{\bar{\omega}}{v}[z^2 + (y-b)^2]^{1/2}\right) ,$$

and $\bar{\omega}(v)$ is determined by the random stopping power S_r due to one electron:

$$S_r = \rho \int db\, 2\pi b \Delta E(b, v) = \rho \int db\, 2\pi b \Delta E_{\bar{\omega}}(b, v) . \tag{11}$$

In (10) we have introduced Cartesian coordinates $\vec{r} = \{x, y, z\}$ with the x and y axes parallel to $\vec{v}$ and $\vec{b}$ (Fig. 2) and K_n are the modified Bessel functions.[8] In our model we have $\langle \vec{r}|0\rangle = [1/(\pi a_0^3)^{1/2}] e^{-r/a_0}$ where $a_0 = a_B/Z_i$ is the scaled Bohr radius a_B. In the momentum representation, the matrix elements in (10) are

$$\langle 0| V(\bar{\omega})|0\rangle = -\frac{16e^2}{\pi a_0^4} \int \frac{d\vec{k}}{k^2} \frac{e^{-i\vec{k}\cdot\vec{b}}}{(k^2+\kappa^2)^2} \delta(\bar{\omega} - \vec{k}\cdot\vec{v})$$

$$= -\frac{16e^2}{\pi a_0^4 v} \int \frac{d^2k}{k^2+\eta^2} \frac{e^{-i\vec{k}\cdot\vec{b}}}{(k^2+\eta^2+\kappa^2)^2} , \tag{12}$$

where

$$\eta = \bar{\omega}/v, \quad \kappa = 2/a_0 .$$

The $\vec{k}$ integration in (12) has to be performed in the plane perpendicular to $\vec{v}$. Similarly we have

$$\langle 0| \, |V(\bar{\omega})|^2 |0\rangle = \frac{16e^4}{\pi^2 a_0^4 v^2} \int \frac{d^2k_1}{k_1^2+\eta^2} \frac{d^2k_2}{k_2^2+\eta^2} \frac{e^{i(\vec{k}_1 - \vec{k}_2)\cdot\vec{b}}}{[(\vec{k}_1 - \vec{k}_2)^2 + \kappa^2]^2} . \tag{13}$$

For the following the space representation of (13) will be useful also. With (10) we obtain

$$\langle 0| \, |V(\bar{\omega})|^2 |0\rangle = \frac{4e^4}{\pi a_0^3 v^2} \int d\vec{r}\, e^{-2r/a_0} K_0^2(\eta[z^2 + (y-b)^2]^{1/2})$$

$$= \frac{e^4}{\pi v^2} \int d^2x\, x K_1(x) K_0^2\left(\frac{\eta}{\kappa}|\vec{x} - \kappa\vec{b}|\right). \tag{14}$$

The integration area in (14) is the y, z plane.

For the determination of $\bar{\omega}$ according to (10) and (11), we have to square (12) and integrate it as well as (13) over all impact parameters. This yields a δ function in $\vec{k}$, which reduces the two $\vec{k}$ integrations to only one:

$$S_r = (4\rho\bar{\omega} e^4/\hbar v^2)\{I_1 - I_2\} , \tag{15}$$

where

$$I_1 = \int \frac{d^2k}{(k^2+\eta^2)^2} = \frac{\pi}{\eta^2} , \quad I_2 = \frac{2^8}{a_0^8} \int \frac{d^2k}{(k^2+\eta^2)^2 (k^2+\eta^2+\kappa^2)^4} ;$$

substituting $1/x = 1 + k^2/\eta^2$ in I_2 results in

$$I_2 = \frac{\pi}{\eta^2} \int_0^1 \frac{dx\, x^4}{(x + \eta^2/\kappa^2)^4} = \frac{4(\eta/\kappa)^6 + 10(\eta/\kappa)^4 + \frac{22}{3}(\eta/\kappa)^2 + 1}{(\eta^2/\kappa^2 + 1)^3} - \frac{4\eta^2}{\kappa^2} \ln\left(1 + \frac{\kappa^2}{\eta^2}\right)$$

$$\cong \frac{\pi}{5} \frac{\kappa^8}{\eta^{10}} , \qquad \frac{\kappa}{\eta} \ll 1$$

$$\cong \frac{\pi}{\eta^2}\left\{1 + \frac{4\eta^2}{\kappa^2} \ln\frac{\eta^2}{\kappa^2}\right\} , \quad \frac{\kappa}{\eta} \gg 1 . \tag{16}$$

With (16) one obtains for the random stopping power (15)

$$S_r = \frac{4\pi e^4}{\hbar\bar{\omega}(v)} \rho \qquad v \ll \bar{\omega}(v) a_0$$

$$= \frac{4\pi e^4}{mv^2} \rho \frac{m\bar{\omega}(v)}{\hbar} a_0^2 \ln\frac{4v^2}{\bar{\omega}^2 a_0^2} \qquad v \gg \bar{\omega}(v) a_0 . \tag{17}$$

On the other hand, using (11), (4), and (5) S_r is

$$S_r = \hbar\rho \int_0^\infty \omega \sigma_\omega(v)\, d\omega , \tag{18}$$

where the cross section for energy transfer $\hbar\omega$ is

$$\sigma_\omega = \sum_n \delta(\omega - \Delta\omega_n)\sigma_n , \quad \Delta\omega_n = \omega_n - \omega_0 .$$

After Fourier-transforming the Coulomb potential and performing the time integral, (9) can be written

$$f_n = -\frac{ie^2}{\pi\hbar} \int \frac{d\vec{k}}{k^2} \delta(\Delta\omega_n - \vec{k}\cdot\vec{v}) F_n(\vec{k}) e^{-i\vec{k}\cdot\vec{b}} , \tag{19}$$

with

$$F_n(\vec{k}) = \langle n| \, e^{i\vec{k}\cdot\vec{r}} |0\rangle .$$

Then we obtain with (6) and (5),

$$\sigma_n = \frac{4e^4}{\hbar^2 v} \int \frac{d\vec{k}}{k^4} \delta(\Delta\omega_n - \vec{k}\cdot\vec{v}) |F_n(\vec{k})|^2 . \tag{20}$$

Averaging over the magnetic sublevels, the $|F_n(\vec{k})|^2$ are isotropic in $\vec{k}$ and the angular integration in (20) can be performed

$$\langle\sigma_n\rangle = \frac{8\pi e^4}{\hbar^2 v^2} \int \frac{dk}{k^3} \Theta(1 - (\Delta\omega_n/kv)^2) \langle| F_n(k)|^2\rangle \tag{21}$$

with the step function

$$\Theta(x) = \begin{cases} 1, & x > 0 \\ 0, & x < 0 . \end{cases}$$

Introducing (21) into (18) yields

$$\sigma_\omega = \frac{8\pi e^4}{\hbar^2 v^2} \int \frac{dk}{k^3} \Theta(1 - (\omega/kv)^2) S(k, \omega) \tag{22}$$

with the inelastic structure factor

$$S(k, \omega) = \sum_n \delta(\omega - \Delta\omega_n) |F_n(\vec{k})|^2 . \tag{23}$$

S is the probability for transferring the energy $\hbar\omega$ to the bound electron after a momentum transfer $\hbar\vec{k}$. With the closure relation one can easily prove the following sum rules[9]:

$$\int S(k, \omega) d\omega = 1 ,$$

$$\int \omega S(k, \omega) d\omega = \langle\omega\rangle_k = \frac{\hbar k^2}{2m} , \tag{24}$$

$$\int \omega^2 S(k, \omega) d\omega = \langle\omega^2\rangle_k = \langle\omega\rangle_k^2 (1 + 4/3a_0^2 k^2) .$$

Using (22) we obtain from (18),

$$S_r = \frac{8\pi e^4}{\hbar v^2} \rho \int \frac{dk\, d\omega\, \omega}{k^3} \Theta\left(1 - \left(\frac{\omega}{kv}\right)^2\right) S(k, \omega). \tag{25}$$

In Fig. 3 we have plotted the $k\omega$ plane together with the integration limit $\omega = kv$ and the parabola $\langle\omega\rangle_k = \hbar k^2/2m$, around which the integrand in (25) is concentrated. The parabola intersects the line $\omega = kv$ at $\hbar k_m = 2mv$, the maximum momentum transfer to a free electron, where with (24) for $v \gg v_0$ $= \hbar/ma_0$ the fluctuations of ω are small. Then momentum transfers $k > k_m$ are negligible for $v \gg v_0$. The minimum momentum transfer occuring in (25) is $k_1 = \Delta\omega_1/v$ (Fig. 3), corresponding to the smallest energy transfer $\hbar\Delta\omega_1$ to the first excited state of the atom. With the fluctuations of ω in (24) one can easily see, that for $v \gg v_0$ energy transfers $\omega > kv$ are negligible and can be included in the ω integration in (25). The exact but tedious calculation by Bethe[1] shows that this induces for hydrogen atoms a change of 30% in the argument of the logarithm in (26) which is negligible for $v \gg v_0$. Therefore we can integrate in (25) over the shaded area of Fig. 3. This results with (24) in

$$S_r = \frac{8\pi e^4}{\hbar v^2} \rho \int_{k_1}^{k_m} \frac{dk}{k} \int \omega S(k, \omega)\, d\omega$$

$$= \frac{4\pi e^4}{mv^2} \rho \ln \frac{2mv^2}{\hbar\Delta\omega_1} . \tag{26}$$

The random stopping power S_r in (26), calculated here by averaging the semiclassical channeling stopping power S_c for one electron over all impact parameters, is identical with the full quantum-mechanical Bethe-Bloch formula.[1] This justifies our approach describing the proton motion by a classical trajectory.

Comparing the high-velocity formula (17) with (26) we obtain

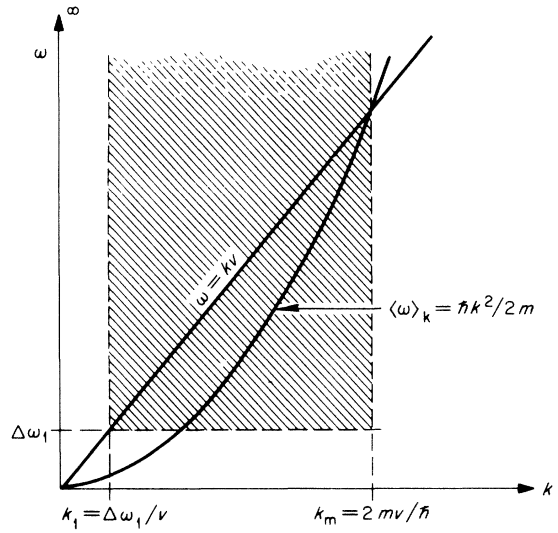

FIG. 3. Energy and momentum transfers contributing to S_r(25).

$$\hbar\bar{\omega}(v \gg v_0) = \hbar^2/ma_0^2 = 2|\epsilon_0| . \tag{27}$$

Since we have no low-velocity approximation for (22), (26), we confine ourselves in the following to fast protons $v \gg v_0$. In contrast to Bloch's $\hbar\bar{\omega}^{B1}$ $= |\epsilon_0|$, Eq. (27) shows that the $\bar{\omega}$ approximation in (10) is consistent with twice the ionization energy. We shall see later that this changes S_c substantially.

The factor two in $\bar{\omega}$ can also be obtained by a different approach. We define the average inelastic excitation energy by

$$\langle\omega\rangle = \frac{\int_{\Delta\omega_1}^\infty \omega\sigma_\omega(v)\, d\omega}{\int_{\Delta\omega_1}^\infty \sigma_\omega d\omega} = \frac{S_r}{\hbar\rho\sigma_{in}} , \quad \sigma_{in} = \int_{\Delta\omega_1}^\infty \sigma_\omega\, d\omega . \tag{28}$$

In the third term of (28) we have used (18) and introduced the total inelastic cross section σ_{in} for one electron. This can be calculated for $v \gg v_0$ from (22) in the same way as S_r. Similarly to the derivation of (26) we obtain with (23), (24),

$$\sigma_{in} = \frac{8\pi e^4}{\hbar^2 v^2} \int_{k_1}^{k_m} \frac{dk}{k^3} \int_{\Delta\omega_1}^\infty S(k, \omega)\, d\omega$$

$$= \frac{8\pi e^4}{\hbar^2 v^2} \int_{k_1}^{k_m} \frac{dk}{k^3} (1 - |F_0(k)|^2) .$$

Introducing the hydrogenlike ground state $\langle\vec{r}|0\rangle$ $= [1/(\pi a_0^3)^{1/2}] e^{-r/a_0}$ in $F_0(k) = \langle 0| e^{i\vec{k}\cdot\vec{r}} |0\rangle$ one obtains after straightforward integration,

$$\sigma_{in} = \frac{4\pi e^4}{\hbar^2 v^2} a_0^2 \ln \frac{8mv^2}{\hbar\Delta\omega_1} . \tag{29}$$

With (28), (26), and (27), this yields

$$\langle\omega\rangle = \hbar/ma_0^2 = \bar{\omega} , \tag{30}$$

so that $\hbar\bar{\omega}$ can be considered as the average inelastic excitation energy.

We now turn back to the explicit b dependence $\Delta E(b, v)$ in (10) and (12)–(14). Performing the angular integration in (12) we have

$$\langle 0|\, V(\omega)\,|0\rangle = -\frac{16e^2}{\pi a_0^4 v}\, i_1 ,$$

$$i_1 = -2\pi\vartheta_{\kappa 2}\int_0^\infty \frac{dk\, k J_0(kb)}{(k^2+\eta^2)(k^2+\eta^2+\kappa^2)} ,$$

where J_0 is the zeroth-order Bessel function.[8] The denominator can be rewritten with the Feynman integral[10]

$$i_1 = -2\pi\vartheta_{\kappa 2}\int_0^1 dx \int_0^\infty dk\, \frac{kJ_0(kb)}{[\kappa^2(1-x)+k^2+\eta^2]^2} .$$

The k integration can be performed,[8] supplying a modified Bessel function K_1, which can be integrated over x after a straightforward substitution, with the result

$$i_1 = -2\pi\vartheta_{\kappa 2}(1/\kappa^2)\{K_0(b\eta) - K_0(b(\kappa^2+\eta^2)^{1/2})\} . \quad (31)$$

For fast protons we can neglect η^2 in (31). Then we obtain for $b\kappa \gg 1$ or $b \gg a_0$, dropping the second term in (31),

$$\langle 0|\, V(\omega)\,|0\rangle \cong -\frac{2e^2}{v} K_0(b\eta), \quad b \gg a_0,\ v \gg v_0 \quad (32)$$

and for small impact parameters $b \ll a_0$, expanding K_0,

$$\langle 0|\, V(\omega)\,|0\rangle \cong \frac{e^2}{v}\left(2\ln\left(\frac{\eta}{\kappa}\right)+1\right) + O(b^2), \quad b \ll a_0,\ v \gg v_0 \quad (33)$$

Similarly we discuss the integral in (14) for large and small b. For $b \gg a_0$ we expand K_0^2 for small x. The linear term drops out because of spherical symmetry. The integrals over x are straightforward with the recurrence relations for the K_n.[8] The result is, for $b \gg a_0$:

$$\langle 0|\,|\, V(\omega)\,|^2|\,0\rangle \cong (4e^4/v^2)\{K_0^2(\eta b) + (4\eta^2/\kappa^2)[K_1^2(\eta b) + K_0^2(\eta b)]\}, \quad b \gg a_0 . \quad (34)$$

For $b \ll a_0$ we drop b in (14) and expand the Bessel function K_0^2 for small argument $\eta/\kappa \ll 1$ or $v \gg v_0$. The integrals over x are evaluated in the Appendix. Then we obtain for

$$\langle 0|\,|\, V(\omega)\,|^2|\,0\rangle \cong \frac{4e^4}{v^2}\left\{\ln^2\frac{\eta}{\kappa} + \ln\frac{\eta}{\kappa} + \frac{\pi^2}{12}\right\} + O(b^2), \quad b \ll a_0,\ v \gg v_0 . \quad (35)$$

With (32)–(35) we obtain from (10) for the average energy loss per electron with binding energy $|\epsilon_0|$ as a function of impact parameter b

$$\Delta E(b, v \gg v_0) \cong 8|\epsilon_0|\left(\frac{v_0}{v}\right)^4\left(\frac{v_B}{v_0}\right)^2\left\{K_1^2\left(\frac{b}{b_c}\right) + K_0^2\left(\frac{b}{b_c}\right)\right\}, \quad b \gg a_0$$

$$\cong 2|\epsilon_0|\left(\frac{v_B}{v}\right)^2(\tfrac{1}{3}\pi^2 - 1), \quad b \ll a_0 \quad (36)$$

$$v_B = \frac{e^2}{\hbar}, \quad b_c = \frac{\hbar v}{2|\epsilon_0|} = \frac{v}{v_0}a_0, \quad \epsilon_0 = \frac{\hbar^2}{2ma_0^2} = \frac{1}{2}mv_0^2 ,$$

where we have introduced the Bohr velocity v_B and a critical impact parameter b_c, $v/b_c = v_0/a_0$ having the intuitive meaning of equal angular velocity of the passing proton and the electron in the orbit.

For the high velocities under consideration ($v \gg v_0$) we have $b_c \gg a_0$. Therefore the large-impact-parameter result in (36) can be expanded:

$$\Delta E(b \gg a_0, v \gg v_0) \cong 8|\epsilon_0|\left(\frac{v_0}{v}\right)^4\left(\frac{v_B}{v_0}\right)^2\frac{b_c^2}{b^2}, \quad a_0 \ll b \ll b_c$$

$$\cong 8\pi|\epsilon_0|\frac{b_c}{b}\left(\frac{v_0}{v}\right)^4\left(\frac{v_B}{v_0}\right)^2 e^{-2b/b_c} ,$$

$$b \gg b_c \gg a_0 . \quad (37)$$

Compared with Bloch's result the small-impact-parameter formula (36) does not show an unphysical divergence at $b = 0$, but stays finite. The integral over all b supplies the Bethe-Bloch formula without an artificial cutoff at small b. The critical impact parameter b_c is a factor of 2 smaller than Bloch's b_c, reducing the range of $\Delta E(b)$ by one-half, while the magnitude of $\Delta E(a_0 < b < b_c)$ is increased by a factor of 2.

The important feature of (36) and (37) is that for high proton velocity $v \gg v_0$ the main contribution to the b-integrated energy loss is supplied by large impact parameters $a_0 \ll b \lesssim b_c$, corresponding to protons traveling at a large distance from the electron distribution. This is because of the small $1/b^2$ decrease, which in the total stopping is weighted with $2\pi b$ and provides the log term in the Bethe-Bloch formula. The long-range behavior is due to the Coulomb potential V, which leads to a long-range inelastic dipole interaction of the passing proton with the target atom. Therefore the stopping of fast ions in matter is not related to the local electron density, which as shown in the following has drastic consequences for the reduction of S_c as compared to S_r.

Breaking the k integration in (26) in one part from k_1 to $k_2 = 1/a_0$ and a second from k_2 to k_m, one obtains equal contributions for small ($k < 1/a_0$) and large ($k > 1/a_0$) momentum transfers, which roughly corresponds to excitation and ionization. A similar equipartition occurs in Lindhard's dielectric approach for the energy loss of fast protons in a free-electron gas, corresponding to plasmon and single-particle excitation. It has been argued[2] that in a channeling situation, where the ion explores only low electron densities, the single-particle ex-

citations or ionization processes are suppressed and hence the energy loss in the high-energy limit is reduced to one-half by equipartition. This picture uses the local electron density as the basic quantity for single-particle excitations and infers that the large momentum transfers or ionization processes are supplied by $b \leq a_0$ contributing one half to S_r. In contrast to this, (36) shows that not only excitation but also ionization processes correspond to a long range. However this is enhanced by the $\bar{\omega}$ approximation (10), (27), and (30), which overestimates $\Delta E(a_0 < b < b_c)$. On the other hand, the adiabacity criterion supplies critical impact parameters $b_k \cong v/\Delta\omega_k > a_0$ for ionization to states of energy $\hbar\omega_k < \hbar v/a_0$. This supports the long-range behavior of (36), leading to the prediction

$$R(v \to \infty) = (S_c/S_r)(v \to \infty) \geq \tfrac{1}{2} \ . \tag{38}$$

In order to test (38) by a channeling experiment the protons have to be fast enough to meet the requirement $b_c \gg a_0$ and $b_c \gg a$ (Fig. 1) for all electron shells which can be excited by random impact. This is discussed quantitatively in Sec. IV for protons channeled in Si. Electron shells contributing to S_r with $b_c \ll a$ are not or hardly excited under channeling conditions, so that $R(v) \leq R(v \to \infty)$.

For the intermediate impact parameter range $b \cong a_0$, the explicit b dependence of $\Delta E(b, v)$ must be obtained numerically. Equations (10) and (12)–(14) can be put into the form

$$\Delta E(b, v) = \frac{32\epsilon_B v}{\pi v_0}\left[\int_0^\infty \rho^2 K_1(\alpha\rho)\, d\rho \int_0^\pi \{K_0[f(\rho, \phi)]\}^2 d\phi - \frac{\alpha^5}{2\pi\gamma^2}\left\{\int_0^\infty \rho^2 K_1(\gamma\rho) d\rho \int_0^\pi K_0[f(\rho, \phi)] d\phi\right\}^2\right] , \tag{39}$$

where

$$f(\rho, \phi) = (\rho^2 + \beta^2 - 2\beta\rho\cos\phi)^{1/2}, \quad \alpha = 2v/v_0,$$

$$\beta = b/v, \quad \gamma^2 = 1 + \alpha^2 ,$$

and $\epsilon_B = e^2/2a_B$ is the Rydberg constant for hydrogen (13.6 eV).

Numerical evaluation of (39) used Gaussian quadrature methods for both inner and outer integrals. The results are plotted in Figs. 4 and 5, which show the slow decrease of $\Delta E(b, v)$ with b for $v \gg v_0$. From Fig. 4b, one sees that for each b there is a small and a large velocity with the same energy loss. This is also shown by the intersections of two v curves at a single b in Fig. 4a.

III. APPLICATION TO STOPPING POWER MEASUREMENTS IN Si AND Ge

In Sec. III the theory of Sec. II is applied to the stopping-power measurements of Clark *et al.*[11] for 4-MeV protons in different axial channels of Si and Ge. In either case the lattice type is diamond structure with nearly the same lattice constant of about 5.5 Å, and with four outer valence electrons supplied by each lattice atom. We confine ourselves to the best channeled particles, which move along the channel center and can be selected experimentally by the leading edge of the channeled energy-loss spectra.[11] In a first approximation we neglect oscillations of the protons around the channel axis, so that the impact parameter for the atomic collisions does not change with penetration depth.

The outer four valence electrons are described in the hydrogen model of Sec. II by a binding energy $\epsilon_V = 8$ eV and a scaled Bohr radius $a_V = 0.69$ Å corresponding to the first ionization potential of Si and Ge or the half-width of the valence band plus band gap. For 4-MeV protons $v/v_V \cong 16.4$ and the critical impact parameter $b_V \cong 16.4 a_V \cong 11.3$ Å. Since the maximum channel radius is $r_{\langle 110\rangle} \cong 2$ Å (Fig. 6) belonging to the $\langle 110\rangle$ channel, we have $b_V \gg r$ (any channel) and many atoms around the trajectory contribute with their valence electrons to the energy loss of 4-MeV channeled protons. They therefore supply the random value S_r (26), as discussed in Sec. II, so that only the binding energy ϵ_V and not the wave functions of the valence electrons enter in the channel stopping power. Hence our simplified model, describing the hybrid structure of the valence electrons by hydrogenlike ground states, is not reflected in the stopping power value. We shall see below, that for 4-MeV the core electrons have b_c values too small to be excited by the best channeled particles in $\langle 110\rangle$ channels. With the atomic density $\rho \cong 5\times10^{-2}$ (4.4×10^{-2})/Å^3 for Si (Ge) (26) yields therefore with four valence electrons for the stopping power in $\langle 110\rangle$ channeling

$$S_c^{\langle 110\rangle} = 4S_r^V \cong 0.84(0.74) \text{ eV/Å}$$

for Si (Ge) in reasonable agreement with the experimental result 0.68(0.70) (eV/Å).

The next inner shell contains in Si 8 L electrons bound with about 100 eV and in Ge 18 M electrons bound with 50–150 eV. The hydrogenlike model and the theory in the preceding section are too crude to aim at an accuracy of more than 10%. Hence it is sufficient to use an average $\epsilon_{L(M)} \cong 100$ eV for the L (M) shell in Si (Ge), since the results discussed below are not sensitive with respect to $\epsilon_{L(M)}$. Then the scaled Bohr radius is $a_{L(M)} \cong 0.2$

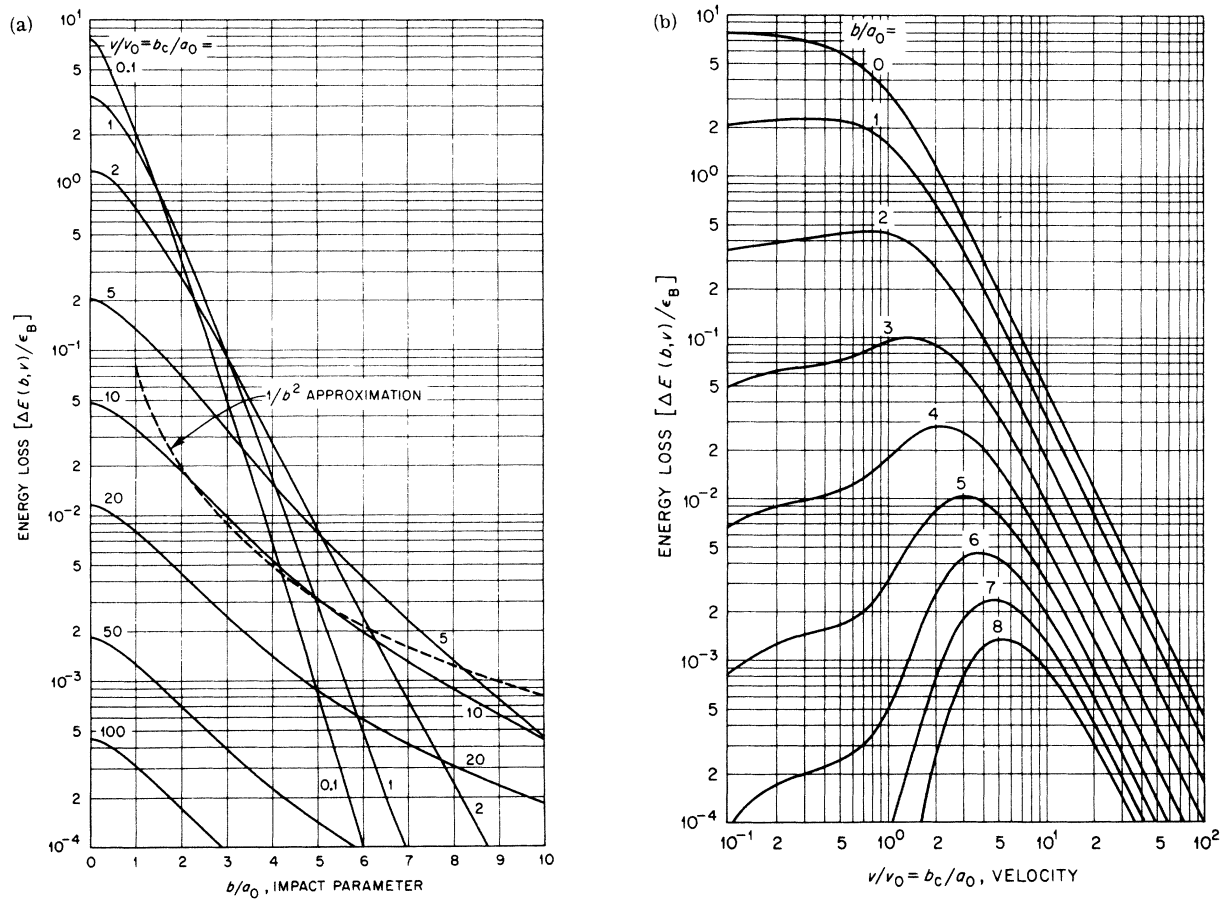

FIG. 4. Average energy loss for a proton-atom collision. The dashed curve shows the asymptotic $1/b^2$ dependence for $a_0 \ll b \ll b_c$ for the case $v/v_0 = 10$.

Å, $v/v_{L(M)} \cong 4.7$, and the critical impact parameter $b_{L(M)} \cong 0.9$ Å. This is half the value following from Erginsoy's adiabaticity criterion[3] which is identical with Bloch's b_c. We neglect the innermost shells, the K shell in Si and the K and L shells in Ge, since they contain fewer and more tightly bound electrons than the two outer shells.

The random contribution due to the 8 (18) L (M) electrons in Si (Ge) is, with (26),

$$8\ (18)\ S_r^{L(M)} \cong 1\ (2.1)\ \text{eV/Å}\ .$$

The most open channel is in the ⟨110⟩ direction with a channel radius $r_{\langle 110\rangle} \cong 2$ Å $> b_{L(M)}$ (Fig. 6). Therefore the best-channeled 4 MeV-protons in the ⟨110⟩ direction do not excite the L (M) electrons in Si (Ge) and we have

$$R_{\langle 110\rangle}(4\ \text{MeV}) = \frac{S_c^{\langle 110\rangle}}{S_r^{\langle 110\rangle}}(4\ \text{MeV}) = \frac{4S_r^V}{4S_r^V + 8(18)S_r^{L(M)}} = 0.46(0.26)\ ,$$

in excellent agreement with the experimental values $R_{\langle 110\rangle} = 0.43(0.28)$ for Si (Ge) by Clark *et al.*[11] Using for $\epsilon_{L(M)}$ 50 or 150 eV instead of 100 eV the theoretical result for $R_{\langle 110\rangle}$ changes only by 10%. This is due to the weak log dependence of $S_r^{L(M)}$ in (26) on $\epsilon_{L(M)} \cong \hbar\Delta\omega_1$. Clearly the asymptotic value (38) is not yet reached for 4-MeV protons. since the core electrons with $b_{L(M)}(4\ \text{MeV}) \cong 0.4\ r_{\langle 110\rangle}$ do not contribute to $S_c^{\langle 110\rangle}$ for the best-channeled protons. The difference of $R_{\langle 110\rangle}$ for Si and Ge contradicts Lindhard's equipartition rule. In our approach the difference R is explained quantitatively by the different electron numbers in the L shell of Si and M-shell of Ge.

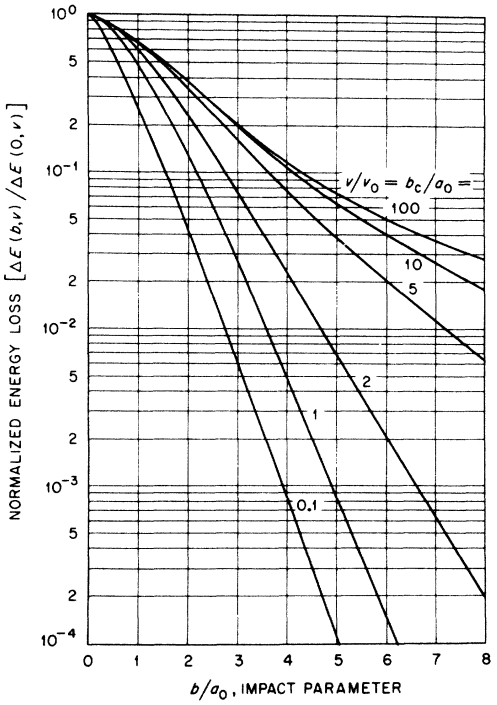

FIG. 5. Normalized average energy loss for a proton-atom collision.

The channel radius $r_{\langle 111\rangle} \cong 1$ Å is determined by the smaller dimension of the $\langle 111\rangle$ channel so that the L (M) shell of Si (Ge) with $b_{L(M)} \cong 0.9$ Å should slightly be excited by the best-channeled particles in the channel. The experimental data of Clark[11] show an increase of 0.2(0.4) eV/Å for $S_c^{\langle 111\rangle}$ with respect to $S_c^{\langle 110\rangle}$.

The ratio of the different increase in Si and Ge $0.2/0.4 \cong 8/18$ is again roughly determined by the 8 (18) electrons in the L (M) shell. With $\Delta E(b, v \cong 4.7 v_{L(M)})$ of (36) we have with 0.42 atoms/Å owing to the two nearest rows of atoms contributing in the smaller $\langle 111\rangle$ channel dimension

$$S_c^{\langle 111\rangle}(4\ \text{MeV}) \cong 4 S_r^{\gamma}(4\ \text{MeV}) + 0.42 \times 8(18) \times 0.23 \left\{ K_1^2\left(\frac{b}{b_{L(M)}}\right) + K_0^2\left(\frac{b}{b_{L(M)}}\right) \right\} . \quad (40)$$

The observed increase of 0.2(0.4) eV/Å is supplied by the second term in (40) for $b \cong 1.2 b_{L(M)} \cong 1$ Å, which corresponds to the trajectory along the center of the $\langle 111\rangle$ channel.

IV. CONCLUSIONS

The theory of Sec. II, based on the impact parameter treatment of an inelastic proton-hydrogen atom collision, has been scaled to Si and Ge and yields good agreement with the experimental results. In particular, it accounts well for the observed ratio R of channel to random stopping power, the difference for Si and Ge being due to the different numbers of electrons in the Si-L and Ge-M shell. The poor hydrogenlike wave functions are not reflected in the results where we apply them, since in all channels the valence electrons supply the random Bethe-Bloch value and the best-channeled particles excite the $L(M)$ electrons in Si (Ge) only for $b \geq b_c$, where the details of the wave functions do not enter. Also the $\bar{\omega}$ approximation (10) influences ΔE mainly for $b \ll b_c$, which can be achieved by the best-channeled protons and the L (M) shells of Si (Ge) only with substantially higher energies. A promising experiment to investigate $R(v \to \infty)$ would be the channeling of about 160-MeV protons in Si, where the L-shell energy is $\epsilon_L \cong 100$ eV and the corresponding critical impact parameter $b_L \cong 5.8$ Å. This is $4.3\, r_{\langle 100\rangle}$, so that the L shell of the Si atoms should be excited for $\langle 100\rangle$ channeling with an efficiency comparable to random conditions. Further calculations to improve the $\bar{\omega}$ approximation are in progress.

ACKNOWLEDGMENTS

We should like to thank G. Leibfried and G. Dearnaley for many stimulating discussions.

APPENDIX

The evaluation of Eqs. (10) and (12)–(14) for impact parameter $b = 0$ requires evaluation of the two integrals

$$D_K(\tfrac{1}{2}e^{\gamma}) = \int_0^{\infty} x^2 \ln^K(\tfrac{1}{2} x e^{\gamma}) K_1(x)\, dx, \quad K = 1,\ 2, \qquad \text{(A1)}$$

where the expansion of $K_0(x)$ for small argument[8] has been used:

$$K_0(x) \cong -\ln(\tfrac{1}{2} x e^{\gamma}) + O(x^2) ,$$

where $\gamma = 0.577\cdots$ is Euler's constant. The essential step in evaluating (A1) is to note that

$$D_K(\alpha) = \lim_{z \to 0} \frac{d^K}{dz^K}\, \alpha^z G(z) , \qquad \text{(A2)}$$

where

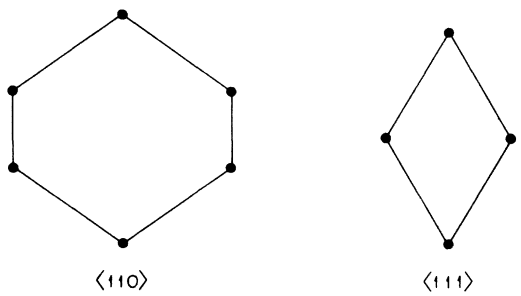

FIG. 6. Cross sections of axial channels in Si and Ge.

$$G(z) \equiv \int_0^\infty x^{z+2} K_1(x)\, dx \,. \tag{A3}$$

Introducing the integral representation[8]

$$K_1(x) = \tfrac{1}{2} x \int_1^\infty (u^2-1)^{1/2} e^{-xu}\, du \,, \tag{A4}$$

and reversing the order of integration, it is easily shown that

$$G(z) = \tfrac{1}{2}\Gamma(\tfrac{3}{2})\Gamma(z+4)\frac{\Gamma(\frac{1}{2}(z+2))}{\Gamma(\frac{1}{2}(z+5))} \,. \tag{A5}$$

Eq. (A5) may now be differentiated as indicated in (A2) and the limiting results are

$$D_1(\alpha) = 1 + 2\ln 2\alpha - 2\gamma \,, \tag{A6}$$

$$D_2(\alpha) = \tfrac{1}{6}\pi^2 + 2\ln^2 2\alpha - 2(2\gamma-1)\ln 2\alpha - 2\gamma(1-\gamma) \,. \tag{A7}$$

Now, with the value $\alpha = \frac{1}{2}e^{\gamma}$, these expressions reduce to the desired results

$$D_1(\tfrac{1}{2}e^{\gamma}) = 1 \,, \tag{A8}$$

$$D_2(\tfrac{1}{2}e^{\gamma}) = \tfrac{1}{6}\pi^2 \,. \tag{A9}$$

---

*Guest scientist, 1971–72. Permanent address: Solid State Division, Oak Ridge National Laboratory, P. O. Box X, Oak Ridge, Tennessee 37830. Research sponsored in part by the U. S. Atomic Energy Commission under contract with Union Carbide Corporation.

[1]H. Bethe, Ann. Physik 5, 325 (1930). H. Bethe, *Handbuch der Physik* (Springer, Berlin, 1933), Vol. 24 I.

[2]J. Lindhard, Kgl. Danske Videnskab. Selskab, Mat.-Fys. Medd. 34, No. 14 (1965).

[3]A. R. Sattler and G. Dearnaley, Phys. Rev. Lett. 15, 59 (1965); B. R. Appleton, C. Erginsoy, and W. M. Gibson, Phys. Rev. 161, 330 (1967).

[4]F. Bloch, Ann. Phys. (Leipz.) 16, 285 (1933).

[5]S. Datz, C. Erginsoy, G. Leibfried and H. Lutz, Ann. Rev. Nucl. Sci. 17, 129 (1967).

[6]M. Kitagawa and Y. H. Ohtsuki, Phys. Rev. B 5, 3418 (1972).

[7]K. Dettmann, Springer Tracts in Modern Physics 58, 119 (1971).

[8]W. Magnus and F. Oberhettinger, *Formeln und Sätze für die Speziellen Funktionen der Mathematischen Physik* (Springer-Verlag, Berlin, 1948).

[9]M. Inokuti, Rev. Mod. Phys. 43, 297 (1972).

[10]J. D. Jackson and H. Schiff, Phys. Rev. 89, 359 (1953).

[11]G. J. Clark, D. V. Morgan, and J. M. Poate, in *Atomic Collission Phenomena in Solids*, edited by D. W. Palmer, M. W. Thompson, and P. D. Townsend (North-Holland, Amsterdam, 1970), p. 388.